

Original Article

Elevated TRIP13 drives cell proliferation and drug resistance in bladder cancer

Sicheng Lu^{1*}, Mengjie Guo^{1*}, Zhimin Fan^{2*}, Ying Chen¹, Xuqin Shi³, Chunyan Gu^{1,2}, Ye Yang^{1,3}

¹School of Medicine and Life Sciences, Nanjing University of Chinese Medicine, Nanjing 210023, Jiangsu, China; ²The Third Affiliated Hospital of Nanjing University of Chinese Medicine, Nanjing 210001, Jiangsu, China; ³School of Holistic Integrative Medicine, Nanjing University of Chinese Medicine, Nanjing 210023, Jiangsu, China. *Equal contributors.

Received March 21, 2019; Accepted June 5, 2019; Epub July 15, 2019; Published July 30, 2019

Abstract: Dysregulation of mitotic processes can induce chromosome instability, which results in aneuploidy, tumorigenesis, and chemo-resistance. Thyroid hormone receptor interactor 13 (TRIP13) is a critical mitosis regulator, and recent studies suggest that it functions as an oncogene in multiple cancers. However, the role of TRIP13 in bladder cancer (BC) is still unknown. In this study, our analysis of RNA-sequencing data from the Cancer Genome Atlas and Gene expression profiling databases showed that TRIP13 expression was upregulated in BC tissues, and overexpression of TRIP13 was significantly associated with poor prognosis of BC patients. In addition, we found a remarkable elevation of TRIP13 in BC samples compared to normal controls by immunohistochemistry. Furthermore, our *in vitro* functional assays showed that overexpression of TRIP13 promoted the growth/viability, colony formation ability by inducing cell cycle arrest in G2/M phase, as well as enhancing drug resistance of BC cells to cisplatin and doxorubicin. Conversely, knockdown of TRIP13 inhibited cell growth and induced apoptosis of BC cells. Furthermore, TRIP13 acted as an oncogene in BC by inhibiting spindle assembly checkpoint signaling by targeting mitotic arrest deficient 2 (MAD2) protein. TRIP13 overexpression also alleviated cisplatin- and doxorubicin-induced DNA damage and enhanced DNA repair as evidenced by the reduced expression of γ H2AX and enhanced expression of RAD50 in drug-treated BC cells. In conclusion, TRIP13 may be a novel target for the treatment of BC.

Keywords: Bladder cancer, TRIP13, oncogene, proliferation, drug resistance

Introduction

Bladder cancer (BC) is a common urinary system malignancy, and it is the 9th most common cancer worldwide [1]. Bladder neoplasias comprise 5% of all diagnosed cancers globally [2]. In 2015, an estimated 74,000 BC cases occurred in the USA, with 16,000 BC-related deaths reported in the same year [3]. Per National Central Cancer Registry of China data, 74,400 newly diagnosed BC cases and 29,400 BC-related deaths were reported in 2013 [4]; notably, 35-45% of these BC patients were identified as having a high risk of recurrence based upon tumor size, grade, multifocality and 10% of them progressed to muscle-invasive disease [5]. For most patients, chemotherapy remains the primary therapeutic strategy to improve quality of life. However, many patients ultimately suffer from poor disease outcomes arising

from chemo-resistance [6]. A previous study has indicated that a complicated molecular mechanism may underlie chemo-resistance in BC [7]. Various urine-based predictive biomarkers exhibit an improved sensitivity in comparison to urinary cytology, but frequently exhibit lower specificity [8-10]. Therefore, exploring novel biomarkers as potential tools for accurately estimating tumor progression and drug resistance in BC is a pressing clinical need.

Thyroid hormone receptor interacting protein 13 (TRIP13) is a member of AAA+ ATPases superfamily characterized by the presence of a conserved nucleotide-binding and catalytic module, the AAA+ module, and is involved in multiple biological processes including spindle assembly checkpoint (SAC) signaling, DNA break formation and recombination, and chromosome synapsis [11, 12]. TRIP13 has been

TRIP13 drives chemo-resistance in bladder cancer

reported to be aberrantly expressed in several primary tumor tissues or cancer cell lines, such as Wilms tumor, primary cutaneous T-cell lymphoma, non-small cell lung cancer, lung adenocarcinoma, breast cancer, prostate cancer, colorectal cancer, squamous cell carcinoma of the head and neck, chronic lymphocytic leukemia, and multiple myeloma [13-26]. However, the role of TRIP13 and its molecular mechanisms of action in BC remain undefined. Among the cast of SAC proteins, Mitotic arrest deficient 2 (MAD2) is identified not only as an inhibitor of SAC signaling [27], but also as a driver of drug resistance in epithelial ovarian cancer [28]. In addition, TRIP13 facilitates double strand breaks (DSBs, the most dangerous type of DNA damage) repair in squamous cell carcinoma of the head and neck [23]. Thus, further studies exploring TRIP13's potential roles in driving tumorigenesis and disease progression in BC are warranted.

In this study, we evaluated the expression levels of TRIP13 in BC tissues and normal control tissues and found a significant association between TRIP13 expression and BC patient outcomes. Then we assessed the role of TRIP13 in influencing the viability, clonogenic capacity, and drug resistance of BC cells *in vitro* and further defined the underlying mechanism of TRIP13's oncogenic functions focusing on the SAC signaling, and drug-induced DNA damage and repair.

Materials and methods

Database analysis

RNA-sequencing data for BC and normal tissues were mined from The Cancer Genome Atlas (TCGA) and the Genotype-Tissue expression (GTEx) database and analyzed in <http://gepia.cancer-pku.cn> [29]. TRIP13 mRNA expression in BC tissues was compared with that in normal bladder tissues. The prognostic value of TRIP13 in BC was evaluated via Kaplan-Meier survival analysis of the BC patients' Gene Expression Profiling (GEP) and outcome data based on Gene Expression Omnibus database.

BC samples and immunohistochemical (IHC) analysis

BC samples for IHC analysis were obtained from Jiangsu Province Traditional Chinese Me-

dicine Hospital. Normal bladder tissue (n=25) and BC tumor tissue (n=75) were used for pathological assessment. The study protocol was approved by the Human Research Ethics Committees of the hospital (Ethics number: 20-19NL-KS27). All patients provided written informed consent for their bladder tissue samples for study use.

The 3 μ m tissue sections were conventionally dewaxed to water, followed by incubation in 3% (v/v) H₂O₂ for 10-15 min to block endogenous peroxidase activity. Then, antigen retrieval was performed using citrate buffer. To block non-specific background staining, 5% BSA was added to the sections, followed by incubation for 5 min at room temperature. Sections were then incubated overnight with anti-TRIP13 primary antibody (Santa Cruz Biotechnology, CA, 1:1,000 dilution) at 4°C, followed by incubation with the secondary antibody for 45 min at 37°C. Tissue sections were then incubated at 37°C for 30 min with StreptAvidin-Biotin Complex (SABC), followed by incubation with the chromogenic substrate 3,3'-diaminobenzidine (DAB) until the desired reaction was achieved. Slides were then counterstained with hematoxylin, dehydrated, and mounted. Semi-quantitative measurements for TRIP13 staining were performed by an experimental pathologist using the following staining intensity scores: 0 indicated no staining; 1+ indicated weak staining; 2+ indicated moderate staining, and 3+ indicated intense staining.

Cell culture

Human bladder cancer cell lines T24 and J82 were purchased from Cell Bank of Chinese Academy of Sciences (Shanghai, China) and were cultured in Dulbecco's Modified Eagle Medium (Biological Industries, Kibbutz Beit Haemek, Israel) supplemented with 10% heat-inactivated fetal bovine serum (Biological Industries, Kibbutz Beit Haemek, Israel), 1% penicillin and streptomycin solution (Sigma, St. Louis, MO), at 37°C in a humidified atmosphere containing 5% CO₂.

Transfection

The sequence of the small interfering RNA oligo targeting TRIP13 (siTRIP13) was as follows: 5'-GCUGAAUCCAUGGGCUUUTAAAGCCCAUGGAAUUCAGCTT-3'.

TRIP13 drives chemo-resistance in bladder cancer

siTRIP13- and TRIP13-overexpressing plasmids were synthesized by Gene Pharma Co., Ltd. (Shanghai, China). pCMV2-C-FLAG-TRIP13 plasmid for overexpressing TRIP13 (TRIP13^{Hi}; reference sequence: BC000404) was purified from *Escherichia coli* bacteria using TIANGEN EndoFree Mini Plasmid Kit II (TIANGEN Biotech Co. Ltd., Beijing, China). When the T24 and J82 cells attained 70-80% confluency, they were seeded into 24-well plates and transfected using 50 nmol/L of siTRIP13/TRIP13^{Hi} plasmid and 25 nmol/L of Lipofectamine 2000 (Invitrogen, Carlsbad, CA). After 4 h, normal complete medium (Biological Industries, Kibbutz Beit Haemek, Israel) was used to culture the transfected cells. After 48 h, the cells were used for subsequent experiments.

Cell viability assay

After incubation in presence of cisplatin (40 μ M) or doxorubicin (1 μ M) [30, 31], cell viability was evaluated using the 3-(4,5-dimethylthiazol-2-yl)-2,5-diphenyltetrazolium bromide (MTT) tetrazolium reduction assay (Sangon Biotech, Shanghai, China), which was performed as previously described [32]. Cells ($3-4 \times 10^3$ cells/well) were inoculated onto 96-well plates. After culturing for 0 h, 24 h, 48 h, and 72 h, the supernatant was removed before adding 10 μ L of 5 mg/mL MTT and 90 μ L of complete medium to each well for 4 h. Afterwards, the medium was removed and 150 μ L dimethyl sulfoxide was added to each well. Finally, the absorbance of the reaction solution was measured at a wavelength of 570 nm using a multi-function microplate reader (Varioskan LUX, Thermo, Manassas, USA).

Flow cytometry

For the apoptosis assay, 1×10^5 T24 or J82 cells were seeded into each well of 6-well plates. After incubation for 24 h, cells were treated with 40 μ M cisplatin or 500 nM doxorubicin. The cells were harvested after 48 h and stained with Annexin-V-Allophycocyanin (Annexin-V-APC)/propidium iodide (PI) apoptosis detection kit (Real-gen Biotechnology, Suzhou, China) according to the manufacturer's instructions. For assay of cell cycle, samples were washed with cold phosphate buffer saline (PBS) twice and fixed in 70% cold ethanol overnight at 4°C, treated with RNaseA (Yeasen, Shanghai, China), then stained with PI for 15 min at room tem-

perature in the dark before analysis. All samples were analyzed using FlowSight (Merck Millipore, Darmstadt, Germany).

Western blot analysis

Protein levels in transfected T24 and J82 cells were detected via western blot analysis. Briefly, total protein was extracted using lysis buffer and was quantified by Microvolume Spectrometer (Berthold, Germany). Next, samples containing about 20 μ g total protein were analyzed by 12/15% sodium dodecyl sulfate-polyacrylamide gel electrophoresis (SDS-PAGE) and transferred onto a polyvinylidene fluoride (PVDF) membrane (Millipore, Bedford, MA). After blocking with 5% non-fat milk, the membrane was incubated with primary antibodies directed against TRIP13 (Santa Cruz Biotechnology, CA, 1:1,000), MAD2 (Santa Cruz Biotechnology, CA, 1:1,000), RAD50 (Cell Signaling Technology, Danvers, MA, 1:1,000), γ H2AX (Cell Signaling Technology, Danvers, MA, 1:1,000), PARP (Cell Signaling Technology, Danvers, MA, 1:1,000), and β -actin (Cell Signaling Technology, Danvers, MA, 1:1,000) at 4°C overnight, followed by incubation with secondary antibodies (Cell Signaling Technology, Danvers, MA, 1:10,000). The bands were visualized by Enhanced Chemiluminescence (ECL) Detection Kit (Amersham Pharmacia Biotech, Piscataway, NJ). The immunostaining band was quantified using Image J software.

Colony formation assay

Colony formation assay was utilized to assess the proliferation and clonogenic growth capacity of BC cells. The assay was been replicated three times. Cells were inoculated onto 6-well plates at the density of 300 cells/well and cultured for 10-14 days. Each cell type was divided into three groups: non-treated, 0.4 μ M cisplatin-treated, and 100 nM doxorubicin-treated cells. Colonies were fixed with 5% glutaraldehyde and then stained with crystal violet. After capturing the images of colonies, colony numbers were analyzed with the help of Image J.

Immunofluorescence assay

The immunofluorescence assay was performed as previously described [33]. Briefly, cells were fixed in 4% paraformaldehyde for 20 min. Then, the samples were treated with 0.2% Triton X-

TRIP13 drives chemo-resistance in bladder cancer

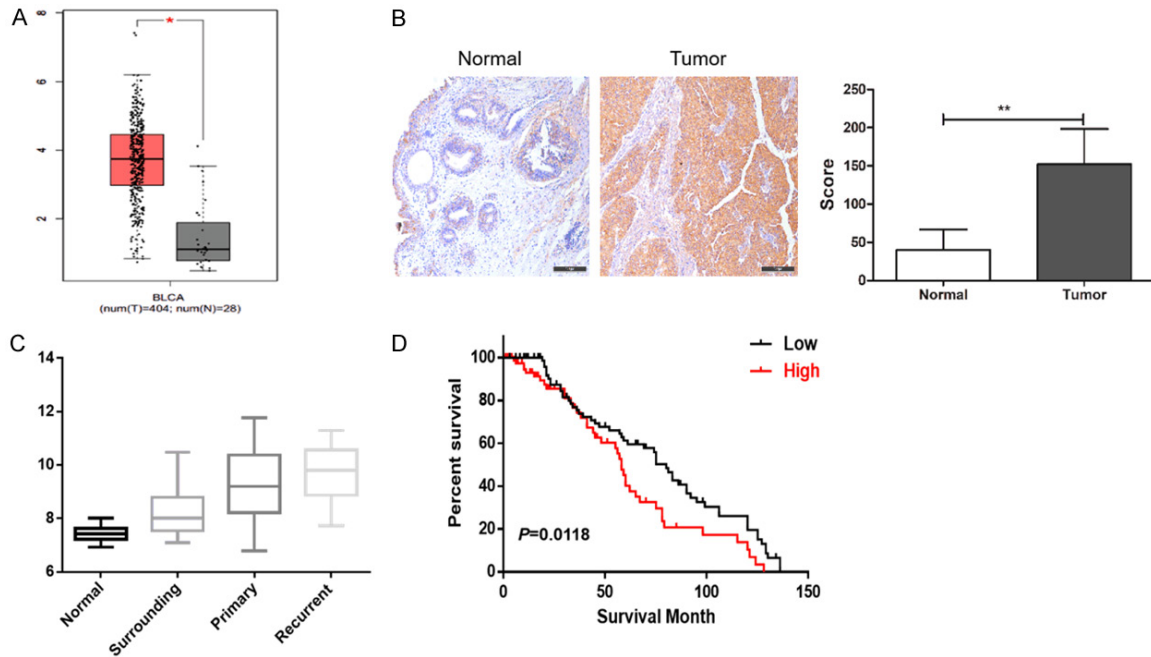


Figure 1. TRIP13 message levels in samples of BC and normal tissues. A. TRIP13 gene expression was markedly increased ($*P < 0.05$) in tumor tissue from BC patients ($n = 404$) compared to normal bladder tissues ($n = 28$) in the TCGA database. B. Representative images and mean IHC staining intensity of TRIP13 protein expression in normal and tumor tissues. C. In GTEx dataset, TRIP13 expression showed a trend of gradual increase from samples of normal looking bladder mucosae with surrounding carcinoma cells, to tumor tissues of patients with primary and recurrent BC. D. Patients with high expression of TRIP13 had poorer overall survival rates ($P = 0.0118$) compared to patients with low TRIP13 level.

100 for 20 min and washed with PBS. After that, samples were blocked with 4% bovine serum, and then incubated with anti- γ H2AX antibody (Cell Signaling Technology, Danvers, MA, 1:200) overnight at 4°C. Subsequently, the samples were incubated with Alexa-labeled secondary antibodies (Alexa Fluor 488, 1:200) for 1 h at room temperature. Lastly, nuclei were stained with DAPI (Solarbio Life Sciences, Beijing, China, 1:1,000). The sections were imaged via confocal microscopy (Optika 500TiFL, Thermo, Manassas, USA).

Statistical analysis

The SPSS 22.0 software and GraphPad prism 5.0 software were employed for statistical analyses and drawing diagrams. The Kaplan-Meier method was applied to plot the overall survival (OS), which was compared between patients with high and low expression of TRIP13 using the log-rank test. The two-tailed Student's t-test was applied to compare two experimental groups for IHC and *in vitro* experiments. All data were presented as the mean \pm standard deviation

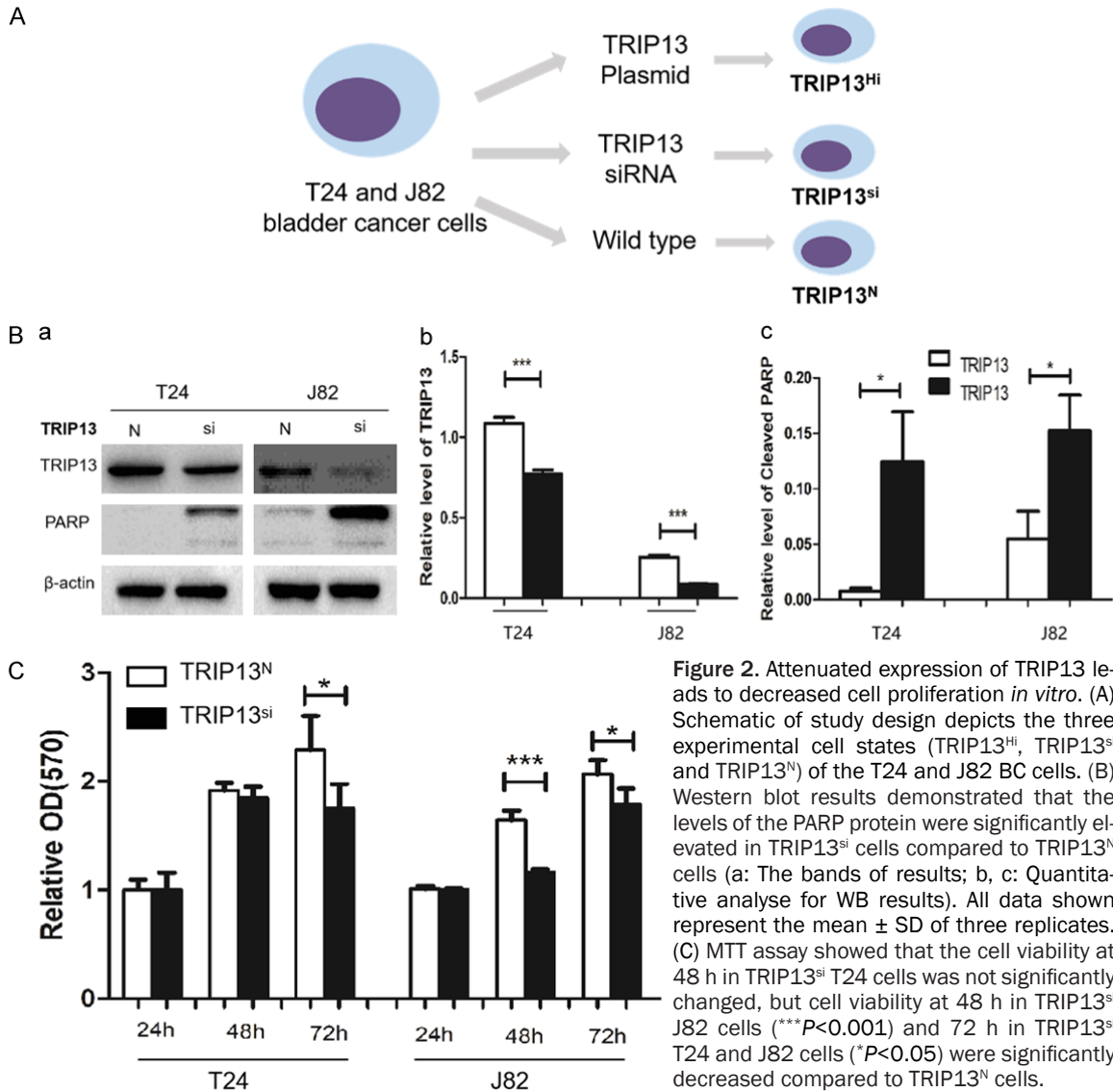
(SD) of three or more independent experiments. The following terminology is used to denote the statistical significance: $*P < 0.05$, $**P < 0.01$, $***P < 0.005$.

Results

Overexpression of TRIP13 is associated with poor overall survival of BC patients

Using RNA-sequencing data downloaded from the TCGA database, we compared the expression of TRIP13 in normal bladder tissue samples (N, $n = 28$) with that in BC samples (T, $n = 404$) to evaluate if dysregulation of TRIP13 expression was associated with development or progression of BC. TRIP13 expression was significantly elevated in BC samples compared to that in normal controls, indicating an association between TRIP13 overexpression and BC tumorigenesis/progression (**Figure 1A**). In addition, protein level of TRIP13 was significantly upregulated in tumor samples from primary and recurrent BC patients compared to samples from normal bladder tissues (**Figure 1B**).

TRIP13 drives chemo-resistance in bladder cancer



Intriguingly, TRIP13 expression was markedly elevated in tumor-infiltrating, normal looking bladder mucosal cells (surrounding) in GTEx database (Figure 1C). TRIP13 overexpression in samples from recurrent patients compared to tumor samples from patients with primary BC suggest overexpressed TRIP13 in BC cells may contribute to drug resistance and cell proliferation (Figure 1C). Additionally, we evaluated the role of TRIP13 in the prognosis of BC patients by Kaplan-Meier survival analysis. BC patients with high TRIP13 expression suffered from worse OS compared to the patients of low TRIP13 expression ($P=0.0118$) (Figure 1D). Together, these data suggest that TRIP13 may be a potential diagnostic and prognostic marker in BC.

Silencing TRIP13 inhibits cell proliferation and induces cell apoptosis

To assess the function of TRIP13 in BC, we used two BC cell lines T24 and J82 as *in vitro* experimental models of BC. The cells either overexpressed TRIP13 (TRIP13^{Hi}) or showed siRNA-mediated knockdown of TRIP13 (TRIP13^{si}), with wild-type cells serving as controls (TRIP13^N). A representative schematic of the experimental design is shown in Figure 2A. Western blot examination validated that expression of TRIP13 in TRIP13^{si} T24 and J82 cells was significantly reduced compared to that in TRIP13^N T24 and J82 cells (Figure 2Ba and 2Bb). PARP expression is an indicator of apoptosis in multiple cancers. As shown in Figure

2Ba and **2Bc**, PARP expression significantly increased in TRIP13^{si} T24 and J82 cells compared to that in TRIP13^N cells ($P < 0.05$). Potential differences in viability of TRIP13^N and TRIP13^{si} cells were evaluated via MTT assay conducted 24 h, 48 h, and 72 h after transfection. TRIP13^{si} cells showed significantly lower cell growth/viability compared to TRIP13^N cells ($P < 0.05$) (**Figure 2C**). These results suggest that TRIP13 is crucial for the viability of BC cells *in vitro*.

Increased TRIP13 accelerates cell growth and promotes cell cycle progression

To further validate the role of TRIP13 in cell proliferation, we overexpressed TRIP13 in two BC cell lines T24 and J82 using transient transfection. Western blot analysis confirmed markedly elevated expression of TRIP13 in TRIP13^{Hi} cells relative to TRIP13^N cells ($P < 0.05$) (**Figure 3A**). As shown in **Figure 3B**, MTT assay indicated that TRIP13^{Hi} cells showed significantly higher cell viability compared to TRIP13^N controls at 72 h (T24 cells, $**P < 0.01$; J82 cells, $***P < 0.001$). These results were consistent with the findings from our TRIP13^{si} experiments. Moreover, flow cytometric analysis demonstrated that upregulation of TRIP13 promoted cell cycle progression (**Figure 3C**). With DNA stained by PI, TRIP13^{Hi} T24 and J82 cells exhibited 5.4% and 8.1% higher proportion of cells in G2/M phases than in TRIP13^N cells, respectively (**Figure 3D**; $*P < 0.05$). **Figure 3E** depicts PI-stained examples of cells in prophase, metaphase, anaphase, and telophase. Together, these findings illustrated that TRIP13 accelerates BC cell growth/viability, which promotes cell entry into mitosis.

Increased TRIP13 expression is associated with drug resistance

Cisplatin and doxorubicin are currently the first-line treatments for BC. We tested the effect of cisplatin and doxorubicin on TRIP13^N and TRIP13^{Hi} cells. After 2 days of cisplatin (concentrations: 0, 10.47, 20.94, 41.88, 83.75, 167.5 and 335 μM) or doxorubicin (concentrations: 0, 1.57, 3.13, 6.25, 12.5, 25 and 50 μM) treatment, the proliferation of TRIP13^N T24 and J82 cells was significantly inhibited relative to TRIP13^{Hi} T24 and J82 cells (**Figure 4A**, top panel). We also observed that the IC₅₀ of cisplatin and doxorubicin in TRIP13^{Hi} cells was much higher compared to TRIP13^N cells when evalu-

ated via the MTT assay (**Figure 4A**, bottom panel). TRIP13^{Hi} T24 and J82 cells treated with 0.4 μM cisplatin (middle panels) or 100 nM doxorubicin (right panels) or untreated (left panels) produced ~15% or ~12% or more colonies respectively, than TRIP13^N controls (**Figure 4B** and **4C**). These results indicate a clear correlation between TRIP13 overexpression and drug resistance. In addition, cell apoptosis was measured by flow cytometry after the apoptotic cells were stained by the APC-conjugated Annexin-V. As shown in **Figure 4D**, after the cells were treated with cisplatin or doxorubicin for 48 h, both TRIP13^{Hi} T24 and J82 cells contained significantly fewer apoptotic cells than TRIP13^N cells ($P < 0.05$), suggesting that TRIP13 overexpression may contribute to the apoptosis-resistance of these drug-treated cells.

TRIP13 acts as an oncogene by inhibiting SAC signaling and drug-induced DNA damage in BC

We focused on SAC signaling pathway and the critical factor MAD2 to explore the potential mechanism by which TRIP13 overexpression may drive BC development/progression. MAD2 protein level in TRIP13^{si} and TRIP13^{Hi} cells was detected by western analyses. As expected, MAD2 expression was significantly decreased in TRIP13^{Hi} cells compared to TRIP13^N cells (**Figure 5A**). Conversely, MAD2 expression was dramatically increased in TRIP13^{si} cells compared to TRIP13^N control cells ($P < 0.05$) (**Figure 5A**). To investigate whether TRIP13 regulates DNA damage and repair in BC, we performed western blot analyses to examine DNA damage indicators in TRIP13^{Hi} and TRIP13^N cells treated with cisplatin (DNA damaging drug). H2AX phosphorylated on serine 139 (γH2AX) is a marker of DNA damage, and RAD50 is involved in DNA repair. Under the condition of cisplatin treatment, we observed remarkable reduction of γH2AX protein and elevation of RAD50 in TRIP13^{Hi} cells compared to TRIP13^N cells ($P < 0.05$) (**Figure 5B**). Additionally, we applied immunofluorescence assay to validate that TRIP13 expression has an impact on γH2AX levels. As illustrated by immunofluorescence staining in **Figure 5C**, consistent with the results of our western blots, fluorescence intensity of γH2AX was much higher in TRIP13^{si} cells than in TRIP13^N cells. Based on these data, we conclude that TRIP13 suppresses drug-induced DNA damage, and promotes DNA repair and apoptosis-resistance in drug-treated BC cells.

TRIP13 drives chemo-resistance in bladder cancer

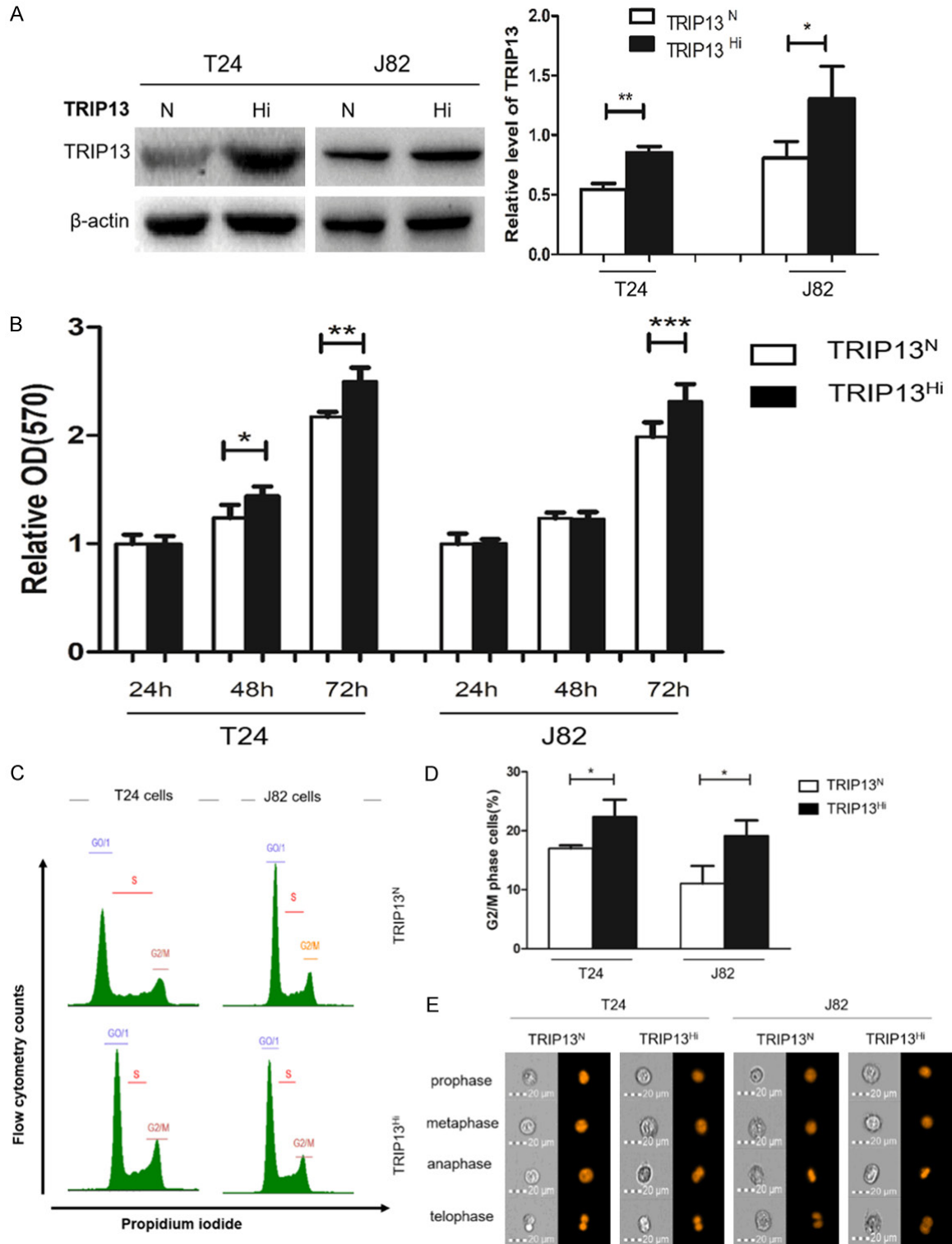
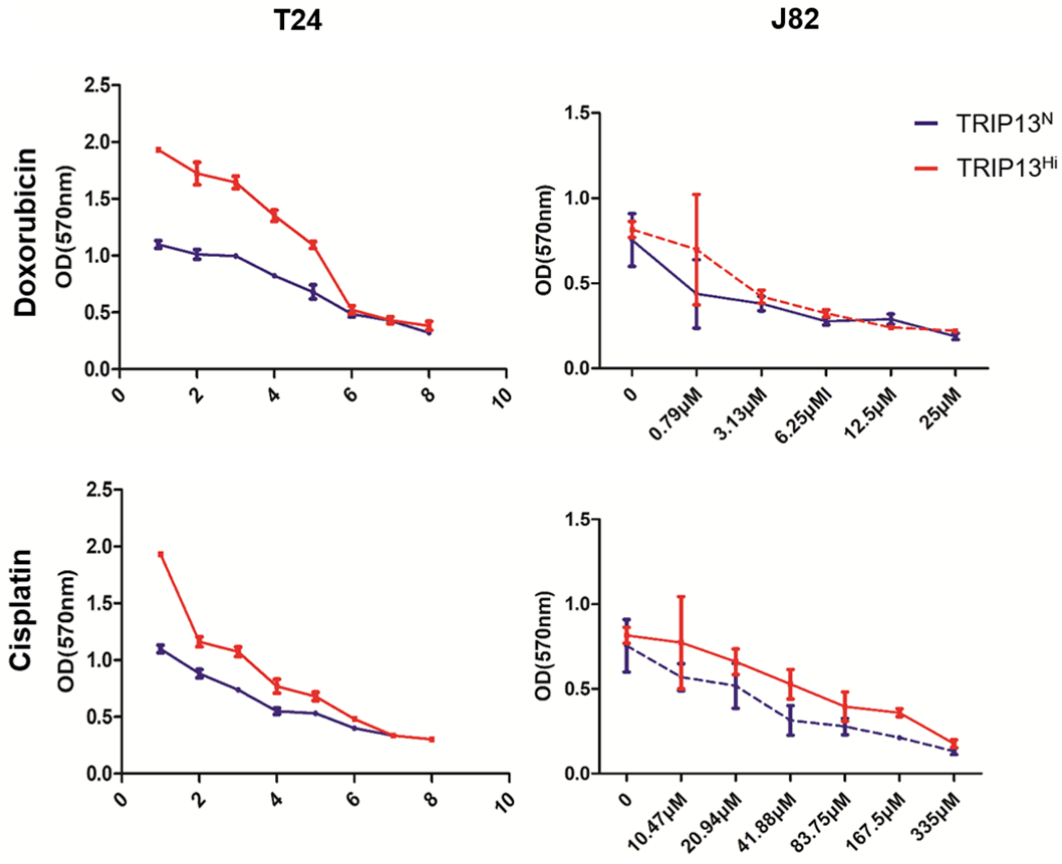


Figure 3. TRIP13 overexpression promotes proliferation of BC cells. **A.** Western blot analysis confirmed that ectopic overexpression of TRIP13 (i.e., the TRIP13^{Hi} BC cell model) was successfully established compared to TRIP13^N cells with significant elevation of TRIP13. These results are representative of three independent overexpression clones. **B.** MTT assay showed that the cell viability at 48 h in TRIP13^{Hi} J82 cells was not significantly changed, but cell viability at 48 h in TRIP13^{Hi} T24 cells (**P*<0.05) and 72 h in TRIP13^{Hi} T24 (***P*<0.01) and J82 cells (***)*P*<0.001) were significantly increased. **C-E.** The distribution of TRIP13^N and TRIP13^{Hi} cells in different phases of the cell cycle was determined by flow cytometry. Elevated TRIP13 led to an increased proportion of cells in G2/M phase in TRIP13^{Hi} cells compared to TRIP13^N cells (**P*<0.05).

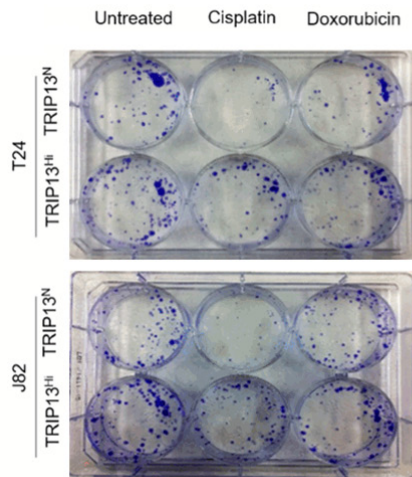
TRIP13 drives chemo-resistance in bladder cancer

A

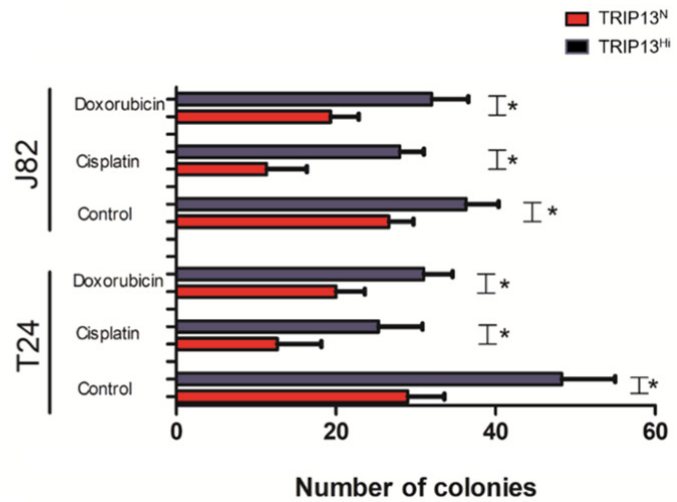


Cells	IC ₅₀ (μM)			
	T24		J82	
	TRIP13 ^N	TRIP13 ^{Hi}	TRIP13 ^N	TRIP13 ^{Hi}
Doxorubicin	0.85	2.41	1.71	4.39
Cisplatin	28.00	47.83	36.60	86.03

B



C



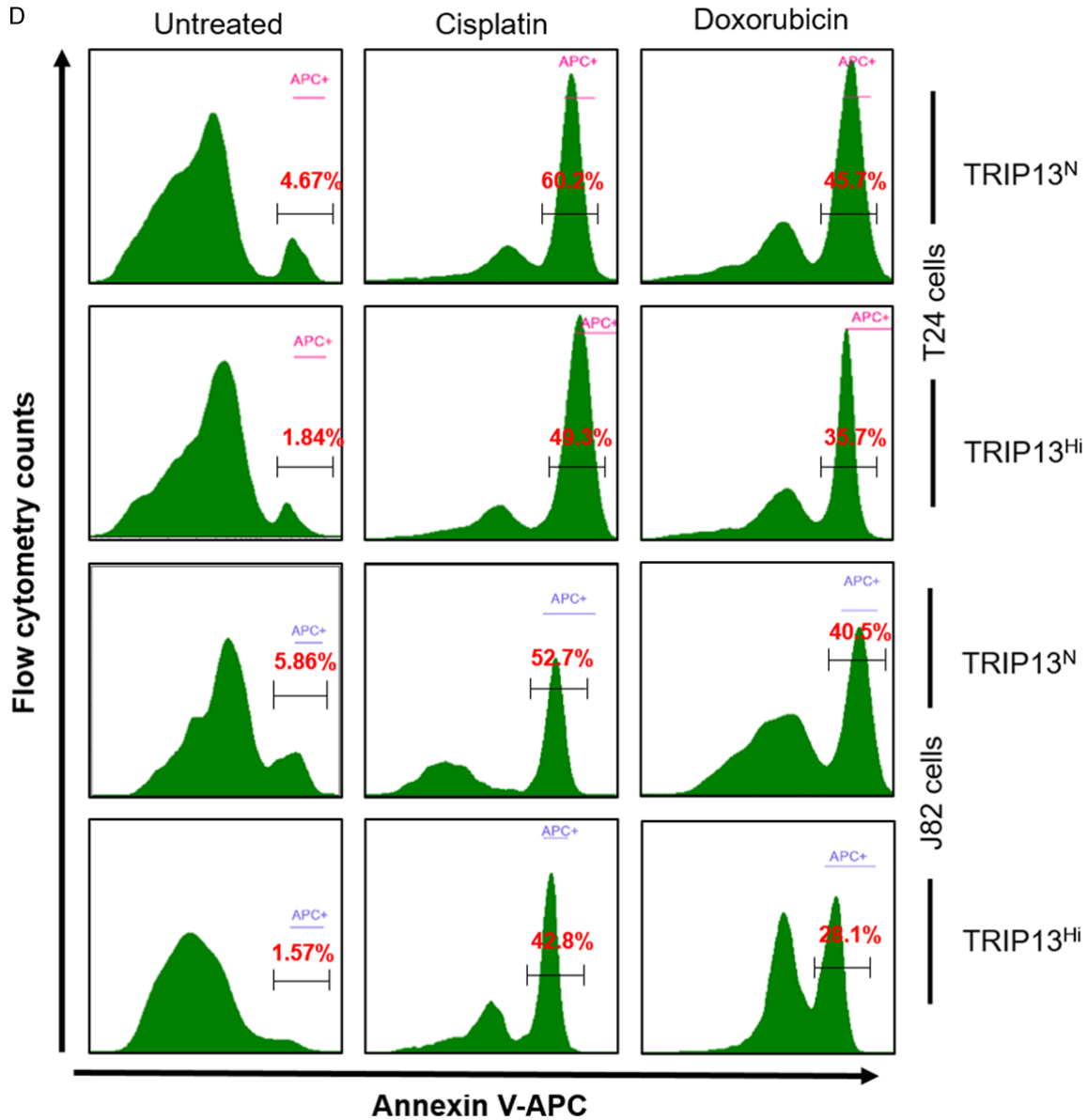


Figure 4. Overexpressed TRIP13 induces cisplatin and doxorubicin resistance in BC cells. A. MTT assay showed that cell viability following cisplatin and doxorubicin treatment for 48 h was much higher in TRIP13^{Hi} cells than that in TRIP13^N cells. B, C. Photomicrographs showing colony formation assay results for untreated control cells (left), cisplatin-treated (0.4 μ M) cells (middle), and doxorubicin-treated (100 nM) cells (right), after 48 h. The average colony numbers of TRIP13^{Hi} and TRIP13^N cells were determined in triplicate experiments and are shown as mean \pm SD. Cisplatin and doxorubicin treatments significantly inhibited colony formation in both TRIP13^{Hi} and TRIP13^N cells ($*P < 0.05$), especially in the latter. D. Flow cytometry illustrated that TRIP13^N T24 and J82 cells showed sensitivity to both the anticancer drugs after a 48 h treatment using the standard apoptotic assay, and the right-shifted peak indicated cells undergoing apoptosis. The TRIP13^{Hi} T24 and J82 cells showed weaker right-shifted peaks compared to TRIP13^N cells ($*P < 0.05$).

Discussion

BC cells have strong proliferative ability and tend to be resistant to chemotherapy, radiation, and biological treatment, which result in rapid tumor growth and a high recurrence rate [34]. As the preferred treatment of BC, cisplatin-

in-based chemotherapy remains more likely to develop drug resistance [35]. Doxorubicin is used as a frontline agent in systemic chemotherapy for BC; however, doxorubicin resistance always leads to treatment failure [36]. Although the molecular mechanism by which TRIP13 promotes drug resistance in BC has not yet been

TRIP13 drives chemo-resistance in bladder cancer

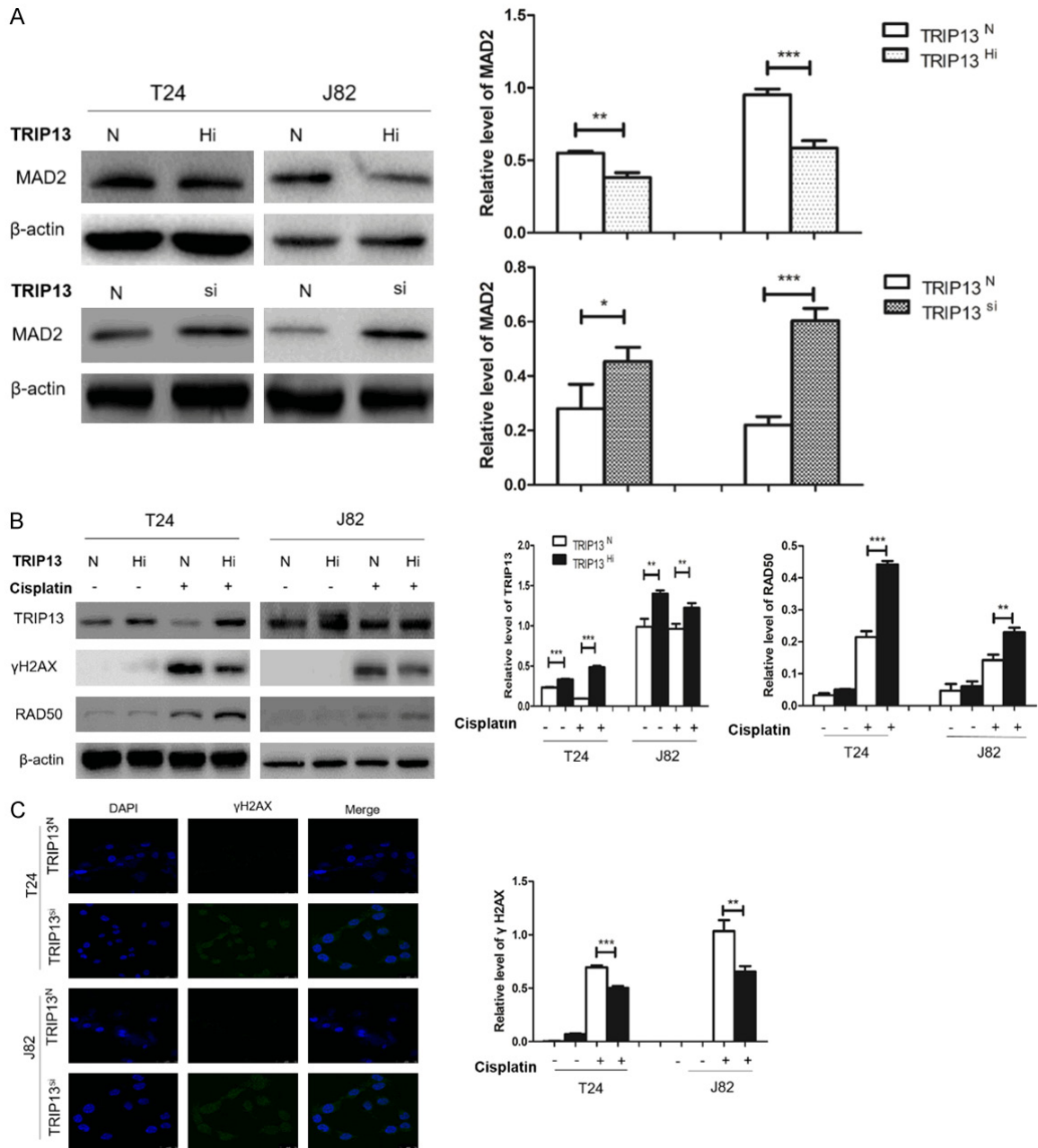


Figure 5. TRIP13 suppresses DNA damage and promotes DNA repair. **A.** The western blot results showed that MAD2 protein level in TRIP13^{Hi} cells was significantly diminished compared to TRIP13^N cells. By contrast, MAD2 was increased significantly in TRIP13^{si} cells compared to TRIP13^N cells. These experiments were repeated three times and representative blots are shown. **B.** Western blot results indicated that the γ H2AX protein levels were markedly down-regulated and RAD50 was significantly upregulated in TRIP13^{Hi} cells compared to TRIP13^N cells treated with cisplatin (40 μ M) for 48 h. These experiments were repeated three times and representative blots are shown. **C.** Immunofluorescence staining of γ H2AX (green) and DAPI (blue; bar =50 μ m) in TRIP13^{si}/TRIP13^N T24 and J82 cells was imaged by confocal microscopy. The results confirmed that increased expression of γ H2AX was seen in TRIP13^{si} cells compared to TRIP13^N cells.

elucidated, TRIP13 misexpression has been implicated in mediating tumor cell proliferation, survival, and invasion in other cancers [20, 25, 37-39].

TRIP13 is located at 5p15.33 and plays an essential role in DNA replication, SAC silencing, and protein degradation [40, 41]. TRIP13 has also been reported to be involved in chromo-

TRIP13 drives chemo-resistance in bladder cancer

some synapsis and meiotic recombination [42]. Interestingly, recent research showed that TRIP13 mutations are present in some tumors, suggesting a potential role for TRIP13 in development or progression of multiple cancers [13, 21, 43]. In prostate cancer, TRIP13 is a predictor of prognosis and functions as a tumor promoter that regulates cell proliferation, invasion, and migration [44]. In multiple myeloma, TRIP13 is associated with poor prognosis (may serve as a prognostic biomarker) and impairs mitotic checkpoint surveillance [25]. In hepatocellular carcinoma, silencing TRIP13 inhibits cell growth and metastasis *in vitro* and *in vivo* [45]. However, there is no research on TRIP13's role in BC. In our study, we found that TRIP13 expression is much higher in BC tissues than in non-tumor bladder tissues. Additionally, elevation of TRIP13 was associated with poor prognosis in BC patients. Functional knockdown of TRIP13 in BC cells resulted in a decrease in the viability of BC cells and apoptosis induction, which is in agreement with the findings in other cancers [21, 23, 25, 38, 39]. Moreover, overexpressed TRIP13 promoted the viability and colony formation capability of BC cells. Drug resistance is still the most important problem in antitumor therapy. Notably, we found that TRIP13 overexpression promotes resistance of BC cells to cisplatin and doxorubicin. Specifically, the half-maximal inhibitory concentration (IC_{50}) of cisplatin was 1.2-fold (T24) and 2.4-fold (J82) higher in TRIP13^{hi} cells compared to TRIP13^N cells, while IC_{50} of doxorubicin was 3.4-fold (T24) and 2.6-fold (J82) higher in TRIP13^{hi} cells compared to TRIP13^N cells. Based on these findings, we propose that upregulation of TRIP13 leads to diminished drug sensitivity, suggesting that TRIP13 may be a good therapeutic target for BC.

To further dissect the signaling pathways through which TRIP13 overexpression may lead to poor outcomes in BC, we analyzed the correlation between TRIP13 expression and MAD2 levels. MAD2 is a SAC protein which functions as a key component of the mitotic checkpoint complex (MCC), which is a suppressor of the anaphase-promoting complex/cyclosome [27]. Moreover, it has been reported that decreased MAD2 may result in drug resistance and tumor cell proliferation in many human cancers [12, 28]. The P13K/AKT signaling pathway, which responds to survival, nutrient metabolism, cell

growth, and apoptosis [46], can positively regulate MAD2 degradation in a multiple myeloma model [25]. Our work showed that forcing TRIP13 overexpression induced degradation of MAD2 and conversely, silencing TRIP13 elevated MAD2 protein levels in BC cells. Enhanced SAC silencing induced by TRIP13 overexpression was associated with an increase in cell proliferation and drug resistance *in vitro*. It has been demonstrated that TRIP13 promotes non-homologous end joining and induces chemo-resistance in head and neck cancer progression [23]. Based on this finding, we evaluated the role of TRIP13 in DNA damage and repair in BC. As γ H2AX is a maker of DSBs, its expression level can be used to quantify DSBs [47]. Our western blot and immunofluorescence analyses suggested that TRIP13 alleviates drug-induced DNA damage (as indicated by a decrease in γ H2AX expression) and promotes DNA repair by enhancing the expression of RAD50. We assert that TRIP13 overexpression promotes the evolution of more aggressive tumor cell phenotypes, including enhanced drug resistance, by enhancing SAC silencing and Mad2 turnover, and thus impairing SAC function in drug-treated cells; impairment of SAC function enhances genetic instability and accelerates evolution of chemo-resistance, metastasis, and leads to poor clinical outcomes, and reducing drug-induced DNA damage, and enhancing DNA repair mechanisms and apoptosis-resistance of drug-treated cells [48, 49].

In summary, our study demonstrates a significant association between TRIP13 overexpression and poor OS of BC patients and provides novel insights into the functions of TRIP13 in growth/viability, clonogenic self-renewal, and drug resistance of BC cells *in vitro*. More studies are warranted to further validate that TRIP13 as a potential therapeutic target in BC.

Acknowledgements

This work was supported by National Natural Science Foundation of China 81770220, 81600177, 81670200 (to CG & YY); The 2016 outstanding youth fund of Jiangsu Province BK20160048 (to YY); Natural Science Foundation of Jiangsu Province BK20161041 (to CG); National Key Research and Development Program: Precision Medicine sub-program 2016YFC0905900 (to YY); The Priority Academic

Program Development of Jiangsu Higher Education Institutions for Chinese Medicine; Innovation Team of Six Talent Peaks Project in Jiangsu Province TD-SWYY-015 (to CG).

Disclosure of conflict of interest

None.

Address correspondence to: Drs. Ye Yang and Chunyan Gu, School of Medicine and Life Sciences, Nanjing University of Chinese Medicine, 138 Xianlin Road, Nanjing 210023, Jiangsu, China. Tel: +86-25-85811597; E-mail: yangye876@sina.com (YY); guchunyan@njucm.edu.cn (CYG)

References

- [1] Tariq A, Khan SR, Vela I and Williams ED. Assessment of bladder cancer patients and carers use of internet, social media and quality of available patient centric online resources: a systematic review. *BJU Int* 2019; 123 Suppl 5: 10-18.
- [2] Moreira JM, Ohlsson G, Gromov P, Simon R, Sauter G, Celis JE and Gromova I. Bladder cancer-associated protein, a potential prognostic biomarker in human bladder cancer. *Mol Cell Proteomics* 2010; 9: 161-177.
- [3] Dobruch J, Daneshmand S, Fisch M, Lotan Y, Noon AP, Resnick MJ, Shariat SF, Zlotta AR and Boorjian SA. Gender and bladder cancer: a collaborative review of etiology, biology, and outcomes. *Eur Urol* 2016; 69: 300-310.
- [4] Chen W, Zheng R, Zhang S, Zeng H, Xia C, Zuo T, Yang Z, Zou X and He J. Cancer incidence and mortality in China, 2013. *Cancer Lett* 2017; 401: 63-71.
- [5] Gingrich JR. Bladder cancer: chemohyperthermia for bladder cancer—clinically effective? *Nat Rev Urol* 2011; 8: 414-416.
- [6] Black PC and Dinney CP. Growth factors and receptors as prognostic markers in urothelial carcinoma. *Curr Urol Rep* 2008; 9: 55-61.
- [7] Mahdavifar N, Ghoncheh M, Pakzad R, Momenimovahed Z and Salehiniya H. Epidemiology, incidence and mortality of bladder cancer and their relationship with the development index in the world. *Asian Pac J Cancer Prev* 2016; 17: 381-386.
- [8] Miyake M, Goodison S, Rizwani W, Ross S, Bart Grossman H and Rosser CJ. Urinary BTA: indicator of bladder cancer or of hematuria. *World J Urol* 2012; 30: 869-873.
- [9] Horstmann M, Todenhofer T, Hennenlotter J, Aufderklamm S, Mischinger J, Kuehs U, Gakis G, Stenzl A and Schwentner C. Influence of age on false positive rates of urine-based tumor markers. *World J Urol* 2013; 31: 935-940.
- [10] Kamat AM, Hegarty PK, Gee JR, Clark PE, Svatek RS, Hegarty N, Shariat SF, Xylinas E, Schmitz-Drager BJ, Lotan Y, Jenkins LC, Droller M, van Rhijn BW and Karakiewicz PI. ICUD-EAU international consultation on bladder cancer 2012: screening, diagnosis, and molecular markers. *Eur Urol* 2013; 63: 4-15.
- [11] Vader G. Pch2(TRIP13): controlling cell division through regulation of HORMA domains. *Chromosoma* 2015; 124: 333-339.
- [12] Miniowitz-Shemtov S, Eytan E, Kaisari S, Sitry-Shevah D and Hershko A. Mode of interaction of TRIP13 AAA-ATPase with the Mad2-binding protein p31comet and with mitotic checkpoint complexes. *Proc Natl Acad Sci U S A* 2015; 112: 11536-11540.
- [13] Yost S, de Wolf B, Hanks S, Zachariou A, Marcozzi C, Clarke M, de Voer R, Etemad B, Uijtewaal E, Ramsay E, Wylie H, Elliott A, Picton S, Smith A, Smithson S, Seal S, Ruark E, Houge G, Pines J, Kops G and Rahman N. Biallelic TRIP13 mutations predispose to Wilms tumor and chromosome missegregation. *Nat Genet* 2017; 49: 1148-1151.
- [14] van Kester MS, Borg MK, Zoutman WH, Out-Luiting JJ, Jansen PM, Dreef EJ, Vermeer MH, van Doorn R, Willemze R and Tensen CP. A meta-analysis of gene expression data identifies a molecular signature characteristic for tumor-stage mycosis fungoides. *J Invest Dermatol* 2012; 132: 2050-2059.
- [15] Kang JU, Koo SH, Kwon KC, Park JW and Kim JM. Gain at chromosomal region 5p15.33, containing TERT, is the most frequent genetic event in early stages of non-small cell lung cancer. *Cancer Genet Cytogenet* 2008; 182: 1-11.
- [16] Rhodes DR, Yu J, Shanker K, Deshpande N, Varambally R, Ghosh D, Barrette T, Pandey A and Chinnaiyan AM. Large-scale meta-analysis of cancer microarray data identifies common transcriptional profiles of neoplastic transformation and progression. *Proc Natl Acad Sci U S A* 2004; 101: 9309-9314.
- [17] Martin KJ, Patrick DR, Bissell MJ and Fournier MV. Prognostic breast cancer signature identified from 3D culture model accurately predicts clinical outcome across independent datasets. *PLoS One* 2008; 3: e2994.
- [18] Nieto-Jimenez C, Alcaraz-Sanabria A, Paez R, Perez-Pena J, Corrales-Sanchez V, Pandiella A and Ocana A. DNA-damage related genes and clinical outcome in hormone receptor positive breast cancer. *Oncotarget* 2017; 8: 62834-62841.
- [19] Larkin S, Holmes S, Cree I, Walker T, Basketter V, Bickers B, Harris S, Garbis S, Townsend P and Aukim-Hastie C. Identification of markers of prostate cancer progression using candi-

TRIP13 drives chemo-resistance in bladder cancer

- date gene expression. *Br J Cancer* 2012; 106: 157-165.
- [20] Dong L, Ding H, Li Y, Xue D, Li Z, Liu Y, Zhang T, Zhou J and Wang P. TRIP13 is a predictor for poor prognosis and regulates cell proliferation, migration and invasion in prostate cancer. *Int J Biol Macromol* 2018; 121: 200-206.
- [21] Sheng N, Yan L, Wu K, You W, Gong J, Hu L, Tan G, Chen H and Wang Z. TRIP13 promotes tumor growth and is associated with poor prognosis in colorectal cancer. *Cell Death Dis* 2018; 9: 402.
- [22] Abdul Aziz NA, Mokhtar NM, Harun R, Mollah MM, Mohamed Rose I, Sagap I, Mohd Tamil A, Wan Ngah WZ and Jamal R. A 19-Gene expression signature as a predictor of survival in colorectal cancer. *BMC Med Genomics* 2016; 9: 58.
- [23] Banerjee R, Russo N, Liu M, Basrur V, Bellile E, Palanisamy N, Scanlon CS, van Tubergen E, Inglehart RC, Metwally T, Mani RS, Yocum A, Nyati MK, Castilho RM, Varambally S, Chinnaiyan AM and D'Silva NJ. TRIP13 promotes error-prone nonhomologous end joining and induces chemoresistance in head and neck cancer. *Nat Commun* 2014; 5: 4527.
- [24] Zhou K, Zhang W, Zhang Q, Gui R, Zhao H, Chai X, Li Y, Wei X and Song Y. Loss of thyroid hormone receptor interactor 13 inhibits cell proliferation and survival in human chronic lymphocytic leukemia. *Oncotarget* 2017; 8: 25469-25481.
- [25] Tao Y, Yang G, Yang H, Song D, Hu L, Xie B, Wang H, Gao L, Gao M, Xu H, Xu Z, Wu X, Zhang Y, Zhu W, Zhan F and Shi J. TRIP13 impairs mitotic checkpoint surveillance and is associated with poor prognosis in multiple myeloma. *Oncotarget* 2017; 8: 26718-26731.
- [26] Heuck CJ, Qu P, van Rhee F, Waheed S, Usmani SZ, Epstein J, Zhang Q, Edmondson R, Hoering A, Crowley J and Barlogie B. Five gene probes carry most of the discriminatory power of the 70-gene risk model in multiple myeloma. *Leukemia* 2014; 28: 2410-2413.
- [27] Pines J. Cubism and the cell cycle: the many faces of the APC/C. *Nat Rev Mol Cell Biol* 2011; 12: 427-438.
- [28] Furlong F, Fitzpatrick P, O'Toole S, Phelan S, McGrogan B, Maguire A, O'Grady A, Gallagher M, Prencipe M, McGoldrick A, McGettigan P, Brennan D, Sheils O, Martin C, W Kay E, O'Leary J, McCann A. Low MAD2 expression levels associate with reduced progression-free survival in patients with high-grade serous epithelial ovarian cancer. *J Pathol* 2012; 226: 746-755.
- [29] Tang Z, Li C, Kang B, Gao G, Li C and Zhang Z. GEPIA: a web server for cancer and normal gene expression profiling and interactive analyses. *Nucleic Acids Res* 2017; 45: W98-W102.
- [30] Raghunathan K, Ahsan A, Ray D, Nyati MK and Veatch SL. Membrane transition temperature determines cisplatin response. *PLoS One* 2015; 10: e0140925.
- [31] Hafeman SD, Varland D and Dow SW. Bisphosphonates significantly increase the activity of doxorubicin or vincristine against canine malignant histiocytosis cells. *Vet Comp Oncol* 2012; 10: 44-56.
- [32] Yang Y, Guan D, Lei L, Lu J, Liu JQ, Yang G, Yan C, Zhai R, Tian J, Bi Y, Fu F and Wang H. H6, a novel hederagenin derivative, reverses multi-drug resistance in vitro and in vivo. *Toxicol Appl Pharmacol* 2018; 341: 98-105.
- [33] Li DJ, Tong J, Zeng FY, Guo M, Li YH, Wang H and Wang P. Nicotinic ACh receptor alpha7 inhibits PDGF-induced migration of vascular smooth muscle cells by activating mitochondrial deacetylase sirtuin 3. *Br J Pharmacol* 2018; [Epub ahead of print].
- [34] Miyamoto DT, Mouw KW, Feng FY, Shipley WU and Efsthathiou JA. Molecular biomarkers in bladder preservation therapy for muscle-invasive bladder cancer. *Lancet Oncol* 2018; 19: e683-e695.
- [35] Martin-Doyle W and Kwiatkowski DJ. Molecular biology of bladder cancer. *Hematol Oncol Clin North Am* 2015; 29: 191-203, vii.
- [36] Guo Y, Zhang H, Xie D, Hu X, Song R and Zhu L. Non-coding RNA NEAT1/miR-214-3p contribute to doxorubicin resistance of urothelial bladder cancer preliminary through the Wnt/beta-catenin pathway. *Cancer Manag Res* 2018; 10: 4371-4380.
- [37] Ye Q, Rosenberg SC, Moeller A, Speir JA, Su TY and Corbett KD. TRIP13 is a protein-remodeling AAA+ ATPase that catalyzes MAD2 conformation switching. *Elife* 2015; 4.
- [38] Kurita K, Maeda M, Mansour M, Kokuryo T, Uehara K, Yokoyama Y, Nagino M, Hamaguchi M and Senga T. TRIP13 is expressed in colorectal cancer and promotes cancer cell invasion. *Oncol Lett* 2016; 12: 5240-5246.
- [39] Li W, Zhang G, Li X, Wang X, Li Q, Hong L, Shen Y, Zhao C, Gong X, Chen Y and Zhou J. Thyroid hormone receptor interactor 13 (TRIP13) overexpression associated with tumor progression and poor prognosis in lung adenocarcinoma. *Biochem Biophys Res Commun* 2018; 499: 416-424.
- [40] Alfieri C, Chang L and Barford D. Mechanism for remodelling of the cell cycle checkpoint protein MAD2 by the ATPase TRIP13. *Nature* 2018; 559: 274-278.
- [41] Brulotte ML, Jeong BC, Li F, Li B, Yu EB, Wu Q, Brautigam CA, Yu H and Luo X. Mechanistic in-

TRIP13 drives chemo-resistance in bladder cancer

- sight into TRIP13-catalyzed Mad2 structural transition and spindle checkpoint silencing. *Nat Commun* 2017; 8: 1956.
- [42] Ye Q, Kim DH, Dereli I, Rosenberg SC, Hagemann G, Herzog F, Toth A, Cleveland DW and Corbett KD. The AAA+ ATPase TRIP13 remodels HORMA domains through N-terminal engagement and unfolding. *EMBO J* 2017; 36: 2419-2434.
- [43] Dong L, Ding H, Li Y, Xue D and Liu Y. LncRNA TINCR is associated with clinical progression and serves as tumor suppressive role in prostate cancer. *Cancer Manag Res* 2018; 10: 2799-2807.
- [44] Dong L, Ding H, Li Y, Xue D, Li Z, Liu Y, Zhang T, Zhou J and Wang P. TRIP13 is a predictor for poor prognosis and regulates cell proliferation, migration and invasion in prostate cancer. *Int J Biol Macromol* 2019; 121: 200-206.
- [45] Yao J, Zhang X, Li J, Zhao D, Gao B, Zhou H, Gao S and Zhang L. Silencing TRIP13 inhibits cell growth and metastasis of hepatocellular carcinoma by activating of TGF-beta1/smad3. *Cancer Cell Int* 2018; 18: 208.
- [46] Gasparri ML, Besharat ZM, Farooqi AA, Khalid S, Taghavi K, Besharat RA, Sabato C, Papadia A, Panici PB, Mueller MD and Ferretti E. MiRNAs and their interplay with PI3K/AKT/mTOR pathway in ovarian cancer cells: a potential role in platinum resistance. *J Cancer Res Clin Oncol* 2018; 144: 2313-2318.
- [47] Li AY, Boo LM, Wang SY, Lin HH, Wang CC, Yen Y, Chen BP, Chen DJ and Ann DK. Suppression of nonhomologous end joining repair by overexpression of HMGA2. *Cancer Res* 2009; 69: 5699-5706.
- [48] Shen CX and Houghton P. DNA damage checkpoints control spindle assembly checkpoint by regulating Mad2. *Cancer Research* 2011; 71.
- [49] Lawrence KS, Chau T and Engebrecht J. DNA damage response and spindle assembly checkpoint function throughout the cell cycle to ensure genomic integrity. *PLoS Genet* 2015; 11: e1005150.